Bendable Zeolite Membrane: Rapid Synthesis with Improved Separation Performance

Bo Wang

Abstract

Separation of CO_2 emitted from stationary resources is effective in reducing CO_2 content in the atmosphere, thereby mitigating adverse climate change effects. Currently, there is considerable research on technologies that can capture CO_2 effectively with cost parameters suitable for practical implementation, but most of them are not applicable due to the high cost.[1] Polymeric membranes are the front runners for this application, but have limitations due to an upper bound of selectivity and permeability.[2] Inorganic zeolite membrane in principle, can have selectivity and permeability considerably higher than polymers.[1,3–5] In this study, we present a cost-effective strategy for zeolite growth WITHIN the pores of a polymer support, with crystallization time of an hour, which makes the process compatible with polymer membrane manufacturing. With a thin coating of 200 nm polydimethylsiloxane (PDMS) on the zeolite-polymer composite, gas transport data for CO_2/N_2 separation indicate separation factors of 35-45, with CO_2 permeance between 1600-2200 GPU (1 GPU = 3.35×10^{-10} mol/(m^2·s·Pa)). The synthesis process results in membranes that are highly reproducible towards transport measurements, and exhibit long-term stability. Most importantly, these membranes because of the zeolite growth within the polymer support, as contrasted to conventional zeolite growth on top of a support are mechanically flexible and have the potential to be fabricated into spiral wound module with high surface area and lowered cost. Also, this innovative flexible inorganic membrane platform can be extended to other microporous structures for various applications.

1. Introduction

In 2011, coal fired power plants, as well as other stationary sources emit 22.0 gigatons of CO_2, which is about 65 % of the total CO_2 emission. There are many competing technologies under consideration for capture of the CO_2, including solvent and solid state adsorption, amine scrubbing, carbonate looping and membranes.[1] Even though some of these technologies have been tested on the pilot scale, and efforts are currently ongoing to do so on a commercial scale, more cost effective technologies are needed. Membranes are an attractive alternative, since there is no thermal regeneration process involved.[1] Polymeric membranes have shown promise not only because of their separation properties, but also large scale manufacturability, leading to reduced costs.[6] However, polymeric membranes because of their solution-diffusivity mechanisms of gas separation exhibit an upper bound (Robeson plot) in performance, with selectivity decreasing with increased permeance.[2] Zeolite membranes, on the other hand do not have this limitation.[3] Zeolites are crystalline microporous aluminosilicates with molecular porosity.[7] For example, the faujasite (FAU) family of zeolites have a three-dimensional architecture with 13 Å supercages connected through 7.4 Å windows.[7] Calculations have suggested that using FAU, CO_2/N_2 separation with selectivity exceeding 500 and CO_2 permeance of 10,000 Barrer (1 Barrer = 3.35×10^{-16} mol·m/(m^2·s·Pa)) can be acheived.[3,7] Extensive research is being carried out on zeolite membranes.[4] In most such studies, membranes are grown on porous inorganic supports because of its rigidity.[8] The potential impact of zeolite membranes has not been realized because of the difficulty of synthesizing high performance membranes in a reliable and cost-effective manner.[1,4] Moreover, the long times of synthesis and the brittle nature of the membranes result in 1000-fold higher cost of zeolite membranes over polymeric

membranes.[1,4] Thus, not surprisingly, there is only one example of a commercial use of zeolite membrane for prevaporation application in ethanol/water separation.

2. Experimental

Chemical Ludox SM-30 colloidal silica (SiO_2, 30%), Ludox HS-30 colloidal silica (SiO_2, 30%), Aluminum isopropoxide ($Al(O\text{-}CH(CH_3)_2)_3$, 98%), Tetramethylammonium bromide ($(CH_3CH_2CH_2)_4N(2Br)$, 98%) and Hexadecylamine (HDA, $CH_3(CH_2)_{15}NH_2$) were purchased from Aldrich (Milwaukee, WI, USA). Aluminum hydroxide ($Al(OH)_3$, 76.5%) was purchased from Alfa Aesar. Sodium hydroxide pellet (NaOH, 99.0%) was purchased from Fisher Scientific. Tetramethylammonium hydroxide ($(TMA)_2O(2OH)$, 25% aqueous) was purchased from SACHEM Inc. Polydimethylsiloxane (PDMS) was provided by Wacker Silicones, Inc. Helium (4.5 grade), carbon dioxide (4.0 grade) and nitrogen (4.5 grade) were purchased from Praxair. All chemicals were used as received. Polyethersulfone (PES) 300kDa membrane was purchased from MILLIPORE Biomax. H_2O used in this study was purified by a Millipore ultrapure water system 18MH.

Nanocrystalline Zeolite Y Seeds The clear synthesis solution composition of 30 nm zeolite Y was: 0.048 Na_2O: 2.40 $(TMA)_2O(2OH)$: 1.2 $(TMA)_2O(2Br)$: 4.35 SiO_2: 1.0 Al_2O_3: 249 H_2O, where TMA^+ is tetramethylammonium cations.[9] The silicon source, 26.2 g Ludox HS-30 and 10.46 g TMAOH were mixed in the PP bottle, sealed with parafilm and stirred at room temperature for 30 min before use. The alumina source, 12.5 g aluminum isopropoxide was dissolved in mixture of 76.5 g H_2O and 52.3 g TMAOH solution by heating in a water bath at 70 ^oC. After cooling down to room temperature, 13.1 g TMABr was added to alumina source solution followed by mixing with the silicon source. The clear sol was aged at room temperature

with stirring for 3 days, followed by heating at 100°C in oil bath with stirring for 4 days. In the synthesis process, nanozeolite remained suspended in solution. Nanozeolite Y particles were captured by ultracentrifugation from product mixture and washed until pH of supernatant was 7. Then nanozeolite particles were sodium ion exchanged by stirring the zeolite suspension in 0.1 M NaCl solution overnight. The ion exchanged product was washed with DI water and stored as 1 wt% aqueous stock solution.

Zeolite Y Seed Deposition Nanozeolite deposition on PES support were prepared with vacuum assisted dip-coating. PES supports were soaked in distilled water overnight followed by in isopropanol for 1 hour and in water for 1 hour before use. Before dip-coating, nanozeolite stock solution was ultrasonicated for 1 hour and then diluted with distilled water to the required concentration. In ultrasonication process, water in sonicator needs to be changed every 20 min to keep temperature low. 20 mL of prepared nanozeolite suspension was moved to a crystal dish before use. In dip-coating process, PES support surface was soaked in nanozeolite seed dispersion for 3 seconds. After coating, nanozeolite deposition layer was dried in room atmosphere overnight and stored in plastic sample bags before use.

Zeolite Y Membrane Synthesis Secondary growth of zeolite membrane used gel composition of 8.3 Na_2O: 1 Al_2O_3: 6.4 SiO_2: 483.9 H_2O.[10,11] First, 2.208 g of $Al(OH)_3$ and 7.29 g NaOH were dissolved in 85.24 g H_2O. Then 13.85 g Ludox SM-30 was slowly added into the mixture. The gel was sealed in PP bottle to age for 4 hours at room temperature before use. After aging, the opaque gel was moved to round bottom flask to dehydrate, in which 40 mL of H_2O was removed from the gel in 1 hour. The seeded support was locked in the holder and immerged into the flask after dehydration was complete. Then, 40 mL of H_2O was dripped back evenly into the concentrated gel in 1 hour of rehydration and the synthesis process was completed. After

synthesis, grown membrane was cooled to room temperature slowly by putting in boiling water and cooling water down naturally to room temperature. After that, membrane samples were soaked in pure water to remove exceed ions overnight. Then, membranes were washed with hair brush.

HDA and PDMS Coating Spin coating was used to deposit a thin layer of HDA and PDMS on grown zeolite membrane. To prepare the solution for spin coating, HDA was dissolved in DI water to make 1 mM disperison followed by pH adjustment to 4 with HCl. Fresh PDMS monomer solution had to be prepared each time to prevent the crosslinking of monomers before spin coating. PDMS monomer stock solution was diluted with heptane, followed by addition of cross linker and catalyst with the ratio of 100:1:0.5 (PDMS: Cross linker: Catalyst). Zeolite membrane samples were taped on a flat spin coating support before coating. In spin coating, solution was dropped on the whole area of membrane 3 s before spinning starts. Spinning process consists of 2,000 rpm for 5 s followed by 4,000 rpm for 1 min. After HDA coating, membranes were dried at room temperature before further fabrications. After PDMS coating, membrane sample was polymerized at room temperature overnight before use.

3. Results and Discussions

As shown in Figure 1, zeolites are synthesized within a porous polymer support, with the polymer acting as a scaffold for growth of interconnected zeolite particles. The zeolite synthesis is rapid enough to be compatible with continuous polymer manufacture. Synthesis of membranes with reproducible performance for CO_2/N_2 separation, long term stability, and most importantly, flexibility has been realized. The flexibility aspect is particularly important because of two reasons. Previous studies of zeolites grown on polymer supports were very susceptible to

cracking and loss of transport properties if not maintained in a flat geometry during all stages of membrane fabrication and use.[11] Second, the flexibility of the membrane and its rapid growth within an hour makes it feasible to develop roll to roll manufacturing techniques and large scale fabrication.

The procedure involved deposition of ~ 30 nm nanozeolite seeds into the PES support (dimension 4 cm × 2 cm). The seeded PES was placed in a gel (8.5 Na_2O: 1 Al_2O_3: 10.9 SiO_2: 487 H_2O) from which water (40 v/v %) had been removed in a reflux apparatus (shown in Figure 2). Membrane growth occurred in the dehydrated gel while the water was added back under reflux conditions and completed in 60 minutes.[10,11] The amount of nanozeolite seeds is critical for controlling zeolite growth within PES support, and a concentration of 10 µg/ml was used. Considering that the pore size of PES is ~ 70 nm (porosity 15%), nanozeolite seeds are expected to penetrate into the PES, since a vacuum deposition technique was used for seed loadings. Scanning electron micrograph in Figure 3a shows that after one hour of zeolite growth, there were crystals on the PES support, but it was not a continuous top layer, as is evidenced from the visibility of the porous structure of PES.

Figure 3b is a STEM view of a cross-sectional FIB cut of the membrane, and indicates growth of a material within the membrane. Figures 3c is the S and Si elemental maps. It is evident that a silicon containing species has grown within the pores of the PES (S map is indicative of PES). Diffraction of this region showed crystalline content (Figure 4). Figure 3d is XRD pattern of the membrane, and peaks marked with an asterisk are indicative of growth of FAU zeolite. The PES support was dissolved by N-methylpyrrolidine, and Figure 3e and 3f are the SEM micrographs from a top view, and Figure 3g and 3h are the side views of the material remaining after dissolution. It is clear that a network of zeolite crystals has grown through the

entire PES network, with a three-dimensional interconnectivity between the zeolite crystallites. Detailed connectivity between zeolite crystallites have been clearly characterized by TEM in Figure 3i.

The zeolite polymer support was coated with ~200 nm film of PDMS, and the separation characteristics were evaluated for CO_2/N_2 separation using dry gases for ten independently prepared membranes. Figure 5a is a plot of the transport data (black circles). The average permeance of CO_2 was 1838.2 ± 159.7 GPU with a CO_2/N_2 selectivity of 38.0 ± 2.8. The reproducibility is quite remarkable as compared to typical zeolite membranes. Transport results of this membrane under different feed gas composition and temperature has been shown in Figure 6, and indicate that the separation is arising from the zeolite. More interesting is the fact that the membranes can be bent around a radius of 1.5 inch, as shown in Figure 5b without sacrificing the transport properties (red circles in Figure 5a). We have shown previously that zeolite membranes grown on top of a PES zeolite exhibit large cracks upon similar flexing with complete loss of CO_2/N_2 separation.[11] Figure 5c shows the long-term transport behavior of one of the membranes. As synthesized, both the permeance and the selectivity are low, and increases to reach a steady state after 10 hours. After reaching steady state, the permeance drops about 10% over the 96h hour test, but the selectivity remains constant. The initial increase in transport characteristics is possibly due to the drying of the membrane with time. Zeolites were used as prepared, and are saturated with water. Removal of some of this water is essential for the transport property.[12]

Table 1 lists the transport properties at various stages of the synthesis with the 10 µg/ml seed dispersion coated and grown sample. As synthesized, the sample shows poor separation properties with CO_2/N_2 selectivity of 1.2 and CO_2 permeance of 2635.1 GPU. There are enough

defects between the zeolite crystallites, as well as the zeolite-PES interface. A thin cover layer of silicone rubber does plug these defects, with significant improvement in transport properties. There is an optimum loading level of PDMS at 2 wt%.

The wetting of the hydrophilic zeolite surfaces by hydrophobic PDMS is an important parameter for optimizing transport properties. Treating the zeolite-PES membrane with n-hexadecylamine (HDA) followed by PDMS treatment improved the CO_2/N_2 separation factor to 48.7 ± 3.0 (blue dots in Figure 5a). Surface adsorption of the HDA on the zeolite will lead to preferential interaction of the amino group with the zeolite surface hydroxyl groups, with the hexadecyl chain pointing away from the zeolite, thereby giving it a hydrophobic interface. Such an interface facilitates PDMS wetting of the zeolite surface, both between zeolite particles and zeolite-PES interface. Enhanced void elimination improves gas transport through the zeolite, resulting in higher CO_2/N_2 selectivity.

There have been extensive studies of mixed matrix membranes (MMM), in which zeolite crystallites are dispersed in a polymer matrix.[13] Ideal MMM exhibit transport by gas molecules passing through adjacent zeolite crystallites that set up a percolation path. Under these circumstances, high loading of zeolite crystals in the polymer should promote better zeolite packing.[13] However, even though increasing zeolite loading in the polymer is simple in practice, poorer transport results are obtained since considerable voids exist between zeolite crystallites that are inaccessible to the polymer. Our zeolite membrane is different from MMM, because zeolite crystallites are grown into a three dimensional network, aided by the scaffolding provided by the PES. Inter connection of zeolite crystals significantly improved gas transport through zeolite frameworks.

Another novel feature of the present membrane is the flexibility of the membrane. This leads to reproducible fabrication, and transport properties, as noted in Figure 5a (red circles). Our hypothesis for the bendability of the composite membrane in that the zeolite particles are connected in a network, and bending the membrane does not disrupt the local connection between the crystallites. The residual porosity within the PES also provides room for motion of the interconnected zeolite network.

4. Conclusion

Both the flexibility and the rapid (1 hour) growth of the zeolite-PES composite membrane provides the opportunity to adapt the rapid roll to roll method used for polymer membrane manufacture to the present composite membrane. One visualizes a process where a seeded PES support is rolled through gel, with a residence time of an hour, resulting in the grown zeolite-PES composite that is washed and coated with a PDMS layer. The flexibility of the membranes, coupled with the rapid synthesis time and roll to roll fabrication will significantly lower the costs of manufacture as compared to conventional zeolite membranes.

Reference

1. Pera-Titus, M. Porous Inorganic Membranes for CO2 Capture: Present and Prospects. *Chem. Rev.* **114,** 1413–1492 (2014).
2. Robeson, L. M. The upper bound revisited. *J. Membr. Sci.* **320,** 390–400 (2008).
3. Krishna, R. & van Baten, J. M. In silico screening of zeolite membranes for CO2 capture. *J. Membr. Sci.* **360,** 323–333 (2010).
4. Gascon, J. *et al.* Practical Approach to Zeolitic Membranes and Coatings: State of the Art, Opportunities, Barriers, and Future Perspectives. *Chem. Mater.* **24,** 2829–2844 (2012).
5. Caro, J., Noack, M., Kölsch, P. & Schäfer, R. Zeolite membranes – state of their development and perspective. *Microporous Mesoporous Mater.* **38,** 3–24 (2000).
6. Merkel, T. C., Lin, H., Wei, X. & Baker, R. Power plant post-combustion carbon dioxide capture: An opportunity for membranes. *J. Membr. Sci.* **359,** 126–139 (2010).
7. Auerbach, S. M., Carrado, K. A. & Dutta, P. K. in *Handbook of Zeolite Science and Technology* (NY: Marcel Dekker, Inc., 2003).
8. White, J. C., Dutta, P. K., Shqau, K. & Verweij, H. Synthesis of Ultrathin Zeolite Y Membranes and their Application for Separation of Carbon Dioxide and Nitrogen Gases. *Langmuir* **26,** 10287–10293 (2010).
9. Holmberg, B. A., Wang, H., Norbeck, J. M. & Yan, Y. Controlling size and yield of zeolite Y nanocrystals using tetramethylammonium bromide. *Microporous Mesoporous Mater.* **59,** 13–28 (2003).
10. Severance, M. *et al.* Rapid Crystallization of Faujasitic Zeolites: Mechanism and Application to Zeolite Membrane Growth on Polymer Supports. *Langmuir* **30,** 6929–6937 (2014).
11. Wang, B. *et al.* Rapid synthesis of faujasite/polyethersulfone composite membrane and application for CO2/N2 separation. *Microporous Mesoporous Mater.* **208,** 72–82 (2015).
12. Kusakabe, K., Kuroda, T., Murata, A. & Morooka, S. Formation of a Y-Type Zeolite Membrane on a Porous α-Alumina Tube for Gas Separation. *Ind. Eng. Chem. Res.* **36,** 649–655 (1997).
13. Rezakazemi, M., Ebadi Amooghin, A., Montazer-Rahmati, M. M., Ismail, A. F. & Matsuura, T. State-of-the-art membrane based CO2 separation using mixed matrix membranes (MMMs): An overview on current status and future directions. *Prog. Polym. Sci.* **39,** 817–861 (2014).

Table 1. Gas Transport Measurement Results of Zeolite Membrane Samples

Sample Name	CO_2 Permeance /GPU	N_2 Permeance /GPU	Total Gas Permeance /GPU	CO_2/N_2 Selectivity
PES	3675.4[a]	3118.1[a]	6793.5 [a]	1.2[a]
2%PDMS/PES	938.8	66.9	1005.7	14.0
ZYM/PES	2635.9	2197.9	4833.0	1.2
1%PDMS/ZYM/PES	1315.5	923.7	2239.2	1.4
2%PDMS/ZYM/PES	**1727.8**	**46.1**	**1773.9**	**37.5**
3.5% PDMS/ZYM/PES	601.9	20.7	622.6	29.0
2%PDMS/HDA/ZYM/PES	1589.9	30.5	1620.4	52.2

Gas transport experiments are performed at 25°C with feed gas composition of dry 20% CO_2 + 80% N_2. [a] Data reported in reference.[11]

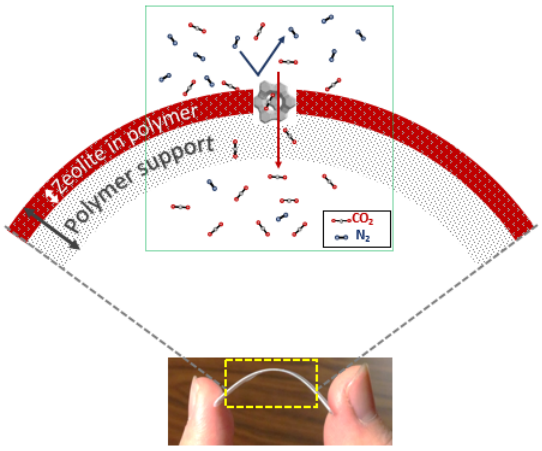

Figure 1. Scheme of bendable zeolite membrane for CO_2/N_2 separation

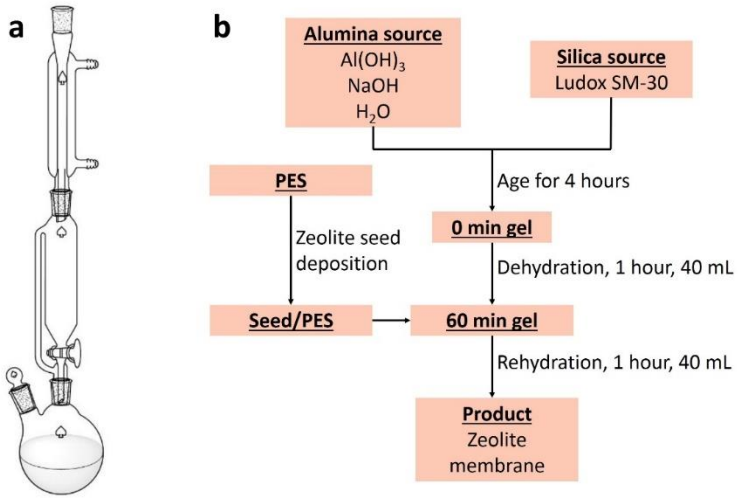

Figure 2. Synthesis procedure of bendable zeolite membrane

a. Reflux apparatus for zeolite membrane synthesis; b. zeolite membrane fabrication process

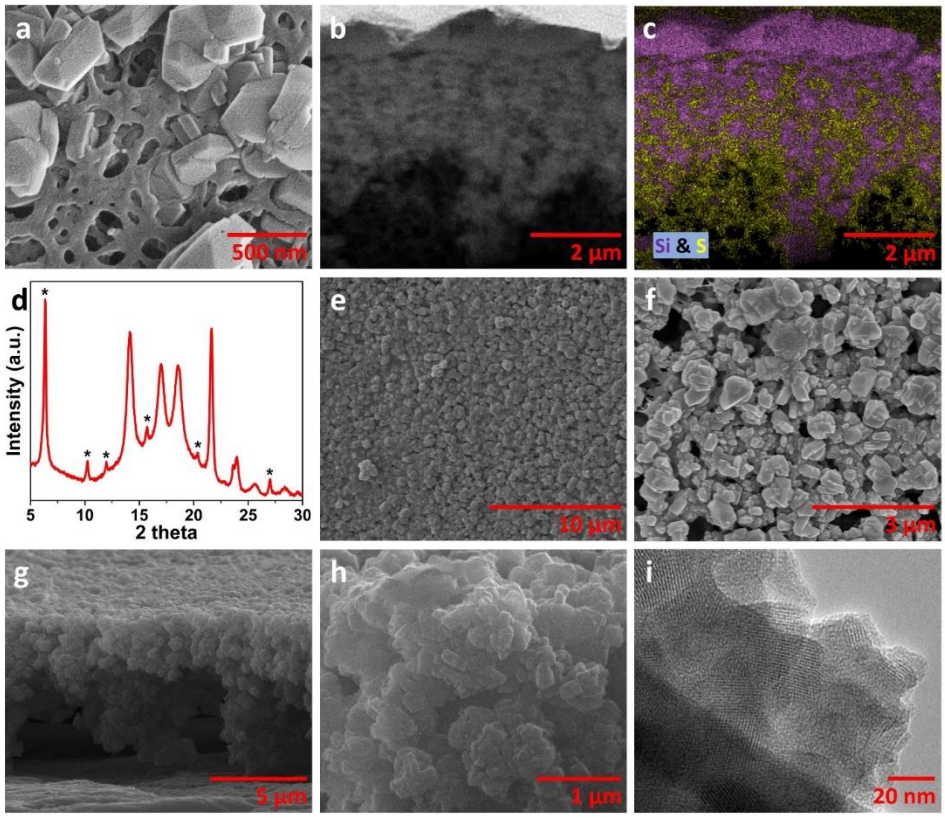

Figure 3. Structural characterization of bendable zeolite membrane

a. top-view SEM of membrane after growth; b. side view STEM of a cross-sectional FIB cut of membrane; c. S and Si elemental maps on a cross-sectional FIB cut of membrane; d. XRD of membrane; e. top view SEM of zeolite layer with PES dissolved; f. high-magnification top view SEM of zeolite layer with PES dissolved; g. side view SEM of zeolite layer with PES dissolved; h. high-magnification side view SEM of zeolite layer close to surface with PES dissolved; i. high magnification TEM images of inter connected zeolite crystallites

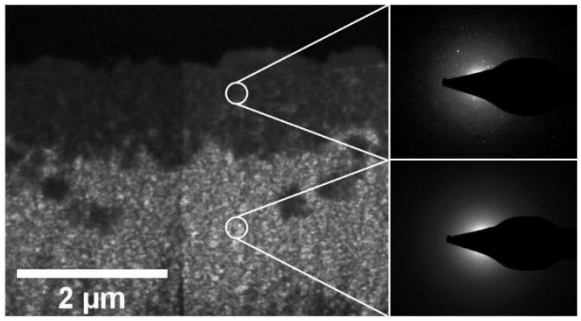

Figure 4. Transmission electron microscopy and diffraction patterns of bendable zeolite membrane

Cross-section TEM of bendable zeolite membrane with diffraction patterns collected at different positions of membrane (top picture shows evidence of crystallinity)

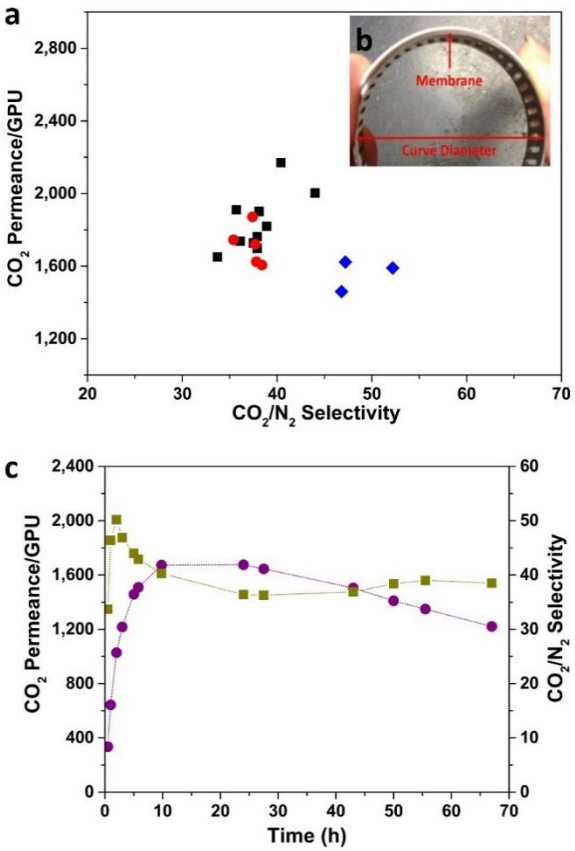

Figure 5. Gas separation performance of bendable zeolite membrane

a. gas transport measurement results of (■) zeolite membrane, as synthesized (●) after bending of membrane and (♦) zeolite membrane coated with HDA; b. picture of membrane bending process; c. long-term (●) CO_2 permeance and (■) CO_2/N_2 selectivity of one of the bendable zeolite membranes zeolite membrane

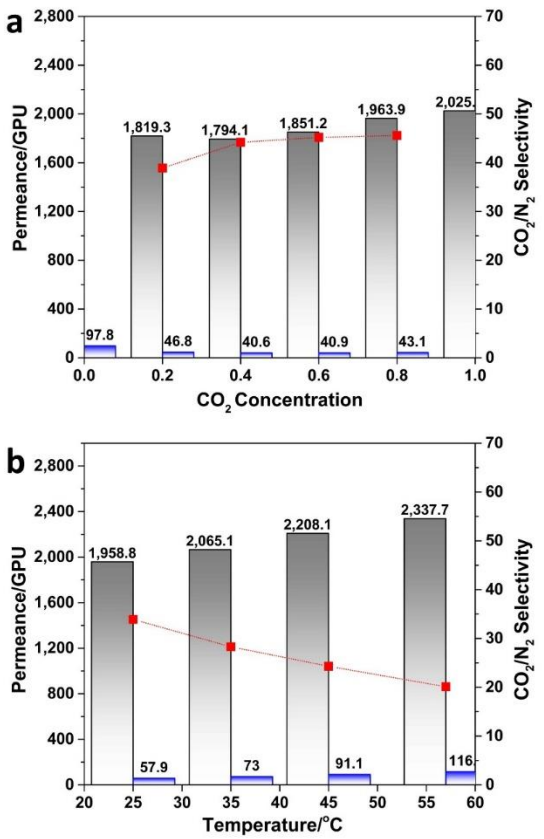

Figure 6. Effect of feed gas composition and temperature on bendable zeolite membranes

Gas separation performance of bendable zeolite membrane (a). with different feed gas compositions and (b). at different temperatures (grey column: CO_2 permeance; blue column: N_2 permeance; red square: CO_2/N_2 selectivity)